Ulf Tengzelius

A Semi-Random Finite Element Modal approach for Turbulent Boundary Layer induced Sound Transmission

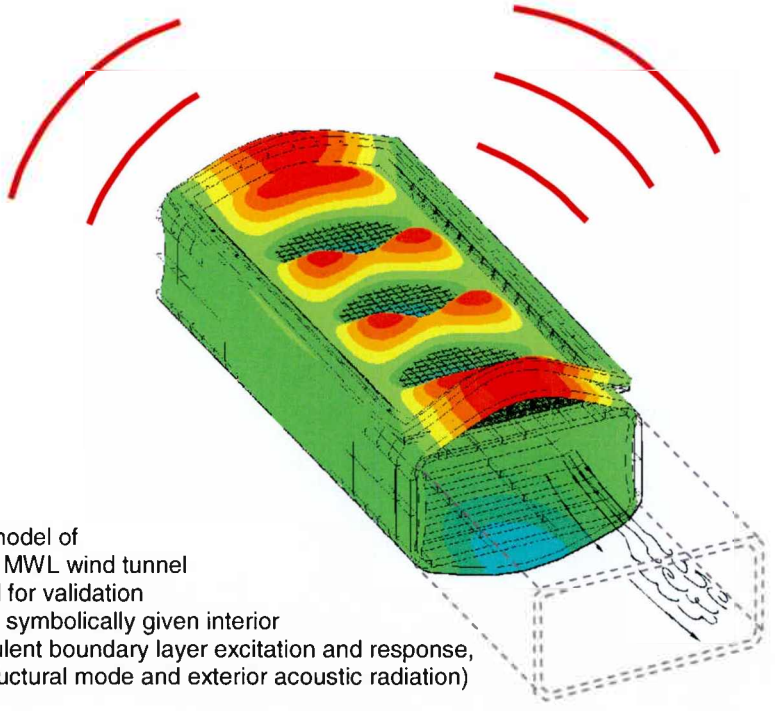

FE model of
KTH MWL wind tunnel
used for validation
(with symbolically given interior
turbulent boundary layer excitation and response,
a structural mode and exterior acoustic radiation)

Titel	-
Title	A Semi-Random Finite Element Modal Approach for Turbulent Boundary Layer Induced Sound Transmission
Rapportnr/Report no	FOI-R--3027--SE
Rapporttyp Report Type	Technical Report
Sidor/Pages	27
Månad/Month	September
Utgivningsår/Year	2010
ISSN	ISSN 1650-1942
Kund/Customer	FM
Projektnr/Project no	E207128
Godkänd av/Approved by	Marlene Johansson

FOI, Totalförsvarets Forskningsinstitut	FOI, Swedish Defence Research Agency
Avdelningen för Försvars- och säkerhetssystem	Defence & Security, Systems and Technology
Flyg- och Systemteknik	Aeronautics and Systems Integration
164 90 Stockholm	SE-164 90 Stockholm

Sammanfattning

En beräkningsmetod som vi benämner "Semi Random Finite Element Method" (SR-FEM), har tagits fram av FOI. Metoden har utvecklats för att kunna prediktera strukturrespons och ljudtransmission från icke deterministiska dynamiska laster på ett effektivt sätt. Föreliggande rapport beskriver metoden och finns också sammanfattad i konferensbidrag, AIAA 2010-3952, till "16th AIAA/CEAS Aeroacoustics Conference" som hölls i Stockholm 7-9 juni 2010.

Finita element (FE) baserade metoder för att beräkna strukturrespons och ljudtransmission från tidsberoende, slumpmässiga, stationära laster, som t.ex. från ett turbulent gränsskikt, har tidigare varit starkt begränsande vad gäller modellstorlek. Redan med relativt små FE modeller, räknat i antalet frihetsgrader, når man tidigt en övre gräns med dagens datorresurser. Med den presenterade metoden förflyttas denna gräns i modellstorlek kraftigt uppåt. Detta medför t.ex. att man, i motsats till tidigare kända modala FE ansatser, ges möjligheten att studera hela flygplanssektioner i frekvensområden upp till flera kHz. Detta svarar bl.a. mot behovet vid beräkningar på flygplanskabiner exciterade av turbulenta gränsskikt.

SR-FEM bygger på en slumpmässig sampling i ingående systemmatriser innan matrismultiplikationer för lösning av struktur- och ljudtransmissionsrespons genomförs. Metoden är generell i den meningen att en godtycklig "stationary random – last " kan appliceras. Till skillnad mot en klassisk modal FE lösning, där de matrismultiplikationer som följer på egenvärdeslösningen kräver avsevärt fler operationer/CPU-tid än egenvärdeslösningen i sig, tenderar dessa båda steg att vara av samma storleksordning med SR-FEM.

Metoden medför en viss begränsning i frekvensupplösning jämfört med en klassisk FE-lösning. För att samtidigt uppnå en avsevärd tidsbesparing (CPU-tid) och "tillräcklig" noggrannhet med SR-FEM, bör man typiskt studera frekvensresponser i tersband. Något som i de flesta sammanhang är fullt acceptabelt. Eftersom SR-FEM är baserad på grundläggande statistiska lagar har man per automatik tillgång till etablerade verktyg för feluppskattning. Detta kan detta t.ex. utnyttjas genom att beräkningar avslutas vid en viss uppnådd noggrannhet.

Nyckelord:

FEM, stationary random, turbulent boundary layer, sound transmission, Monte Carlo Method, sampling, random response, dynamic response, frequency response, FRF

Summary

A method called 'Semi Random Finite Element Method' (SR-FEM) have been developed by FOI. The aim with the SR-FEM has been to extend the capability of classical finite element approaches for responses from stationary random excitations. The following report describe this method , which is summarized in a conference paper, AIAA 2010-3952, given at the "16th AIAA/CEAS Aeroacoustics Conference", Stockholm 7-9th of June 2010.

Finite element (FE) based methods have previously been found quite limited concerning upper model size for computation of structural response and sound transmission from stationary random loads, such as from a turbulent boundary layer. It is well known that when solving a dynamic response problem for deterministic loads, introducing a modal base, the eigenvalue solution is by far the most CPU-time consuming part of the solution process. For a stationary random excitation though, in contrary, the matrix multiplications, following upon the modal base establishment, becomes significantly more costly than the eigenvalue solution. This is when applying a classic modal-FE approach. With the presented SR-FEM instead the CPU-time for this complete set of matrix multiplications tends to be of the same order as the CPU-time for the eigenvalue solution. With this follows that the upper limit in model size could be moved considerably upwards. This enables response studies for example of complete aircraft cabin sections in the frequency range of some kHz, which corresponds to the needs for a typical turbulent boundary layer excitation.

SR-FEM is based on a random sampling among elements within the system matrices established for the computation of structural- or sound transmission response, and is general in the sense that any distributed stationary random load might be applied. The method limits the frequency resolution in relation to a classic FE-solution. In order to achieve a significant CPU-time gain, and at the same time a "sufficient" accuracy, one should typically stay to third octave band representations of the response. In other words, a frequency resolution which can be considered as sufficient in most applications. Since SR-FEM is based on fundamental laws of statistics, means for error estimates is automatically at hand. These error estimates might be used when applying termination criteria for computations. The examples given show an accuracy of around 1 dB per 1/3-octave band compared with a full "classic" modal/FE-approach.

Keywords:

FEM, stationary random, turbulent boundary layer, sound transmission, Monte Carlo Method, sampling, random response, dynamic response, frequency response, FRF

Table of contents

Abbreviations

CFD	Computerised Fluid Dynamics
dof	degrees of freedom
FEM	Finite Element Method
SEA	Statistical Energy Analysis
SR-FEM	Semi Random FEM
TBL	Turbulent Boundary Layer

Denotations

A_j, A_k	areas of finite element j,k
CS	Cross Spectrum
d_{NR}	correction factor for finite population of FE:s
f	force vector
H	transfer function matrix
I_m	confidence interval
I_z	sound intensity in direction normal to surface
k	wavenumber in air
K	stiffness matrix
m^e	mean value
M	panel mass
M	mass matrix
N_{Loop}	Number of outer loop iterations in SR-FEM
NOP_{Exact}	Number of Operations with a standard Modal/FE approach
p	sound pressure
P	sound power
r	space vector to field point in air
$\mathbf{r}_0$	space vector to field point on a vibrating surface
S_0	surface of vibrating area
$\mathbf{S}_{pp}$	pressure cross-spectrum
$\mathbf{S}_{ff}$	force cross-spectrum
$\mathbf{S}^v_{jk}$	plate velocity cross-spectrum
$t_{\alpha/2}$	t-distribution
TP	normalised transmitted soundpower
U_c	convection velocity
u	displacement vector
z	vector of modal displacements
$\mathbf{\Phi}_{pp}$	pressure autospectrum
Γ_{jk}	pressure CS between midpoints of finite element (exterior surface) j and k
ξ_1, ξ_2	spatial separation in 1- and 2-dir.
η	structural damping factor
ω	frequency in radians per second
ω_n	eigen frequency in rad. per second
ψ_n	eigenvector n
φ_n	mass normalised eigenvector n
$\mathbf{\Omega}$	modal receptance matrix
ρ	air density
σ^e	1/3-octave level sample standard deviation

1 Introduction

Good interior cabin noise comfort is a central design goal for modern aircraft. Effective noise reduction on today turbofan engines, a development mainly driven by demands on lower external noise around airports, has improved this comfort substantially. Typically, noise in the cockpit and first half of the cabin in newer aircraft, is dominated by turbulent boundary layer (TBL) noise. Though, in the design process of aircraft cabin wall sections, the TBL noise task has been lacking reliable and efficient tools for: 1) modelling of the TBL wall pressure excitation and 2) the transmission of sound into the cabin.

In this study a method that considers point 2) is proposed, e.g. a method that constitutes a reliable and efficient way to estimate a structural and acoustic response from a given distributed stationary random excitation. This might at a first glance seem as a kind of case which should be possible to solve with standard finite element methods (FEM). This impression is in fact partly true, but only if one look at examples which are very limited in size. The difficulties appear first when one apply these methods to problems of realistic size, let us say a frame section of an aircraft, and find that even super-computers would have problems. This would be the situation both for a mode-based and a direct solution approach. In contrary to modal/FE solutions of problems with deterministic loads, where the eigenvalue solution is the most costly part (in terms of CPU-time or number of operations), the steps following the eigenvalue analysis is by far the most costly part for random excitation problems with distributed loads. The proposed way around this obstacle of long CPU times and limiting upper model size, is to establish a small subset set of degrees of freedom (dof) through a random sampling among all the (physical) dof's of the panel wall surface. Then letting this limited set of dof's be the only ones involved in the computations towards the solution. Different such small sets, which are capable to produce a result with a controlled accuracy, are then run several times. This could be done within a much shorter CPU-time than running the complete set of dof's once. The accuracy, relatively this complete set "exact solution", depends on both chosen computational and presentation frequency bandwidth. It can typically be of the order of 1dB in 1/3-octave bands for a solution that is reached in 1/50 of the time to compute the complete FE model solution.

2 Background

Within ENABLE detailed measurements were carried out on TBL pressure cross-spectra, as well as related vibration response, on a small size panel. Theoretical work in this project focused mainly on two tasks, updating of (at that time) existing models for TBL cross-spectrum and find approaches to circumvent the computer capacity problems related to a direct FE solution of the TBL-noise transmission. Some progress was made regarding characterisation of the TBL pressure fluctuation, but the major step forward were found in the transmission prediction methods. (With results at hand one could state that introducing CFD methods, which it was no room for within ENABLE, would most probably have been beneficial for the further development of TBL pressure models. With the resent strong development of CFD, this is even more emphasized today).

Given specific or more general TBL pressure models, different approaches for the noise transmission were studied in ENABLE. SEA, FEM and different variants of FEM, among them: spectral finite elements and randomised FEM. This paper concentrates on a method of the last type, in the following called SR-FEM, where SR denotes Semi-Random.

The simulation of TBL induced cabin noise remains important, perhaps even more today than before, due to the increasing use of composite materials in aircraft, for which engineers and designers do not have the same experience as for standard aluminium structures.

3 The TBL excitation

A turbulent boundary flow can be characterised as a principal motion, U_1, outside a structural boundary, upon which a random velocity vector, $[u_1, u_2, u_3]$, random in direction and size, is added. Due to the fluid viscosity there is no relative motion between the fluid and the structure at the intermediate surface. When going outwards from the structural surface the relative velocity goes continuously from zero until it reaches the free stream velocity, U_∞. The boundary layer thickness, δ, is usually defined as the distance outside the wall where the flow velocity, $U_1(x_3)$, reaches $0.99U_\infty$, i.e. $U_1(x_3=\delta) = 0.99U_\infty$. This region, with the strong mean velocity gradient outside the surface, is called the boundary layer. The flow induced pressures within the TBL causes vibrations in the structural boundary surface, which in turn radiates sound on both sides. For the sound radiated on the side opposite to the TBL, sound pressure spectra $S_{pp}(\omega, \mathbf{r})$ in Figure 1, we can speak of TBL sound transmission.

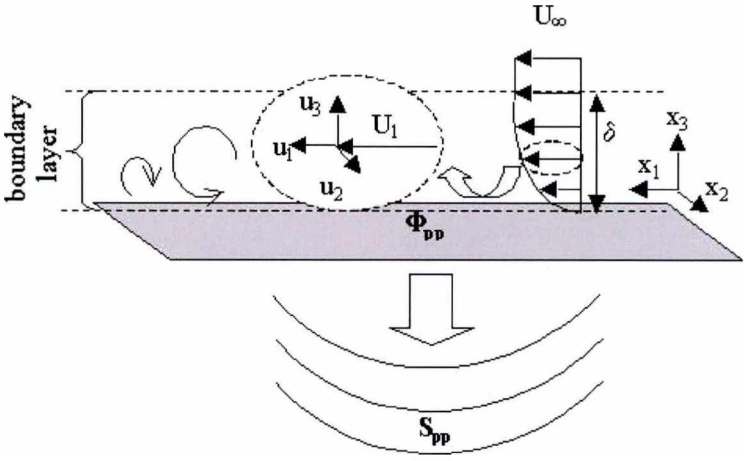

Figure 1. Schematic view of a TBL with some parameters noted together with the sound radiation on the inside of a panel.

In this paper the wall pressure CS, induced by the TBL, is described with the Corcos model [2]. By curve fit from measured spatial correlation between wall pressures Corcos got the following expression for the pressure spectral density in a spatially homogenous TBL:

$$\Gamma_{jk}(\xi_1,\xi_2,\omega) = \Phi_{pp}(\omega) e^{-\alpha_1 \frac{\omega}{U_C}|\xi_1|} e^{-\alpha_2 \frac{\omega}{U_C}|\xi_2|} e^{i\frac{\omega\xi_1}{U_C}} \quad (1)$$

where:
- Φ_{pp} pressure auto spectrum
- ξ_1, ξ_2 spatial separation in 1- and 2-direction, $\xi_1 = x_{1k} - x_{1j}$, $\xi_2 = x_{2k} - x_{2j}$ (1 denotes flow-direction and 2 cross-flow direction , j, k represents wall points j and k respectively)
- U_c convection velocity (characterises the translational speed of the main structures of the turbulence, i.e. the velocity for which the velocity distribution of the turbulence peaks)
- α_1, α_2 constants or ω-dependent functions related to the spatial correlation of he wall pressure spectrum

Several modified variants of this, or other more fundamentally different TBL pressure models can be found in the literature. In the FE/Modal approach outlined in the following, and behind presented results, the Corcos model given in equation (1) has been applied. However, the proposed approach is not limited to the Corcos model, it could easily be replaced by practically any other TBL pressure CS model. For example modifications of equation (1) to non homogenous TBL:s or 2-point cross-spectra established directly from CFD analysis.

4 The TBL response

4.1 Direct FE approach

The starting point here is the assumption that for a discrete structural model the dynamic displacement response of a structure exposed to a deterministic load can be expressed as:

$$\mathbf{u}(\omega) = \mathbf{H}(\omega)\mathbf{f}(\omega) \tag{2}$$

where:
- $\mathbf{u}(\omega)$ is the N×1 displacement response vector given by the finite fourier transform of $\mathbf{u}(t)$
- $\mathbf{f}(\omega)$ is the N×1 force vector, finite fourier transform of $\mathbf{f}(t)$
- $\mathbf{H}(\omega)$ is the N×N transfer function matrix
- N is the number of discrete excitation/response variables (could in the case of a FE model correspond to the number of nodal degrees of freedom)

By employing the relationships between the spectral density function of a stationary random process and the finite fourier transform of this, the displacement response cross-spectral density matrix can be set up outgoing from equation (2) according to [3] :

(I) assume the force cross-spectrum matrix to be given as:

$$\mathbf{S}_{ff}(\omega) = \begin{bmatrix} S_{f_1 f_1} & \cdots & S_{f_1 f_N} \\ \vdots & \ddots & \vdots \\ S_{f_N f_1} & \cdots & S_{f_N f_N} \end{bmatrix} \tag{3}$$

(II) the displacement response cross-spectrum and the force cross-spectrum between degrees of freedom j and k, can be written:

$$S_{u_j u_k}(\omega) = cE\left[u_j(\omega)u_k^*(\omega)\right] \tag{4}$$

$$S_{f_j f_k}(\omega) = c\,E\left[f_j(\omega)f_k^*(\omega)\right] \tag{5}$$

respectively.

where: E denotes an ensemble average over time records
* complex conjugate and
c implies a finite time record of length T such as:

$$cE[f(\omega)g^*(\omega)] \equiv \lim_{T\to\infty} \frac{1}{T} E[f(\omega,T)g^*(\omega,T)]$$

(III) taking the complex conjugate transpose of (2) and post-multiply (2) with this gives:

$$\mathbf{u}(\omega)\mathbf{u}^H(\omega) = \mathbf{H}(\omega)\mathbf{f}(\omega)\mathbf{f}^H(\omega)\mathbf{H}^H(\omega) \tag{6}$$

where H denotes complex conjugate transpose (Hermitian transpose)

(IV) taking the expected value of both sides in eq.(6):

$$cE\left[\mathbf{u}(\omega)\mathbf{u}^{H}(\omega)\right] = \mathbf{H}(\omega)cE\left[\mathbf{f}(\omega)\mathbf{f}^{H}(\omega)\right]\mathbf{H}^{H}(\omega) \quad (7)$$

shows then that the displacement response cross-spectrum matrix may be written:

$$\mathbf{S}_{uu}(\omega) = \mathbf{H}(\omega)\mathbf{S}_{ff}(\omega)\mathbf{H}(\omega)^{H} \quad (8)$$

The transfer function matrices in equation (8) could in principle be derived from a direct FE analysis. As this is a very costly process (see table 1) instead a FE/modal approach will be chosen later.

4.2 Force cross-spectrum matrix

The force CS-matrix (3) can be reached by applying Corcos (1) or some other expression for the TBL pressure CS.. For the sake of computational cost the simplifying alternative of finite element midpoint based force CS matrix , $\mathbf{S}_{ff}$, was chosen in this work. (instead of consistent node related force CS matrix by applying the finite element shape functions). The matrix terms might then be written:

$$S_{f_j f_k} = A_j A_k \Gamma_{jk}(x_1^{(j)}, x_2^{(j)}, x_1^{(k)}, x_2^{(k)}, \omega) \quad (9)$$

where: A_j, A_k areas of finite element j,k

Γ_{jk} TBL pressure CS between midpoints of finite element j and k

The size of $\mathbf{S}_{ff}$ becomes then $N_E \times N_E$, where N_E = number of TBL excited finite elements.

4.3 Modal approach

The transfer function matrix (or frequency response function matrix, FRF-matrix), $\mathbf{H}(\omega)$ introduced in expression (2), can be reached by an inversion of the dynamic system matrix, given by the equations of motion for a discretisized structure:

$$((1+i\eta)\mathbf{K} - \omega^2\mathbf{M})\mathbf{u}(\omega) = \mathbf{f}(\omega) \quad (10)$$

$$\mathbf{H}(\omega) = ((1+i\eta)\mathbf{K} - \omega^2\mathbf{M})^{-1} \quad (11)$$

where: $\mathbf{K}$ is the system stiffness matrix and $\mathbf{M}$ the mass matrix, both with the size $N_{dof} \times N_{dof}$, N_{dof} = number of degrees of freedom
η is the structural damping factor
ω frequency in radians per second

The inversion in (11), or equivalently the solution of (10) with N_{dof} right side $\mathbf{f}$-vectors forming a $N_{dof} \times N_{dof}$ diagonal unitary matrix, needs the order of wN_{dof}^2 operations (w = bandwidth) at each studied frequency. An alternative to this direct method is the modal method. In this latter case a modal base is created by the solution of the reduced eigenproblem without damping [4]:

$$(\mathbf{K} - \omega_n^2 \mathbf{M})\boldsymbol{\psi}_n = \mathbf{0} \tag{12}$$

To each eigenfrequency, ω_n, is related an eigenvector, $\boldsymbol{\psi}_n$, n =1,2…N_{dof} . The complete set of eigenvectors (or modes) compose the full $N_{dof}\times N_{dof}$ modal matrix: $\boldsymbol{\Psi}$, with the modes as column vectors. These eigenvectors are orthogonal with respect to K and M-matrices, i.e.

$$\boldsymbol{\psi}_n^T \mathbf{K} \boldsymbol{\psi}_m = 0 \quad \text{and} \quad \boldsymbol{\psi}_n^T \mathbf{M} \boldsymbol{\psi}_m = 0 \qquad \text{when } n \neq m \tag{13}$$

The amplitude of the modes arising from (12) is arbitrary. A common way of scaling the eigenmodes is a mass normalization, i.e.

$$\boldsymbol{\varphi}_n^T \mathbf{M} \boldsymbol{\varphi}_n = 1 \quad \text{then} \quad \boldsymbol{\varphi}_n^T \mathbf{K} \boldsymbol{\varphi}_n = \omega_n^2 \tag{14}$$

These mass normalized modes sets up the $N_{dof}\times N_M$ modal matrix $\boldsymbol{\Phi}$, where the number of included modes: $N_M \leq N_{dof}$ and typically $N_M << N_{dof}$ after the choosen truncation.

$$\boldsymbol{\Phi}^T \mathbf{M} \boldsymbol{\Phi} = \begin{bmatrix} 1 & & 0 \\ & \ddots & \\ 0 & & 1 \end{bmatrix} = \mathbf{I} \quad \text{and} \quad \boldsymbol{\Phi}^T \mathbf{K} \boldsymbol{\Phi} = \begin{bmatrix} \omega_1^2 & & 0 \\ & \ddots & \\ 0 & & \omega_{N_M}^2 \end{bmatrix} \tag{15}$$

Due to the orthogonallity of the modal base the displacement vector, $\mathbf{u}(\omega)$, can be expressed as:

$$\mathbf{u}(\omega) \approx \boldsymbol{\Phi}\mathbf{z}(\omega) \tag{16}$$

where: $\boldsymbol{\Phi}$ is the truncated modal matrix
$\mathbf{z}$ is a $N_M\times 1$ vector of modal displacements
(also called: mode amplitude or
generalized coordinates or normal coordinates)

Insertion of (16) in (10) and premultiplication with $\boldsymbol{\Phi}^T$ gives:

$$((1 + i\eta)\boldsymbol{\Phi}^T \mathbf{K} \boldsymbol{\Phi} - \omega^2 \boldsymbol{\Phi}^T \mathbf{M} \boldsymbol{\Phi})\mathbf{z}(\omega) = \boldsymbol{\Phi}^T \mathbf{f}(\omega) \tag{17}$$

and when inserting (15):

$$\begin{bmatrix} (1+i\eta)\omega_1^2 - \omega^2 & & 0 \\ & \ddots & \\ 0 & & (1+i\eta)\omega_{N_M}^2 - \omega^2 \end{bmatrix} \mathbf{z}(\omega) = \boldsymbol{\Phi}^T \mathbf{f}(\omega) \tag{18}$$

Equation (18) express N_M uncoupled equations of motion that can be inverted directly:

$$\mathbf{z}(\omega) = \overbrace{\begin{bmatrix} (1+i\eta)\omega_1^2 - \omega^2 & & 0 \\ & \ddots & \\ 0 & & (1+i\eta)\omega_{N_M}^2 - \omega^2 \end{bmatrix}^{(-1)}}^{\boldsymbol{\Omega}(\omega)} \boldsymbol{\Phi}^T \mathbf{f}(\omega) \tag{21}$$

and yielding, with equation (2) and (16), $\boldsymbol{\Phi}\mathbf{z}(\omega) = \mathbf{H}(\omega)\mathbf{f}(\omega)$, where the transfer function matrix (or receptance matrix) , $\mathbf{H}(\omega)$, can be identified as:

$$\mathbf{H}(\omega) = \mathbf{\Phi}\mathbf{\Omega}(\omega)\mathbf{\Phi}^T \tag{22}$$

or alternatively, component wise as a summation:

$$H_{jk}(\omega) = \sum_{n=1}^{N_M} \frac{\varphi_j^{(n)}\varphi_k^{(n)}}{(1+i\eta)\omega_n^2 - \omega^2} \tag{23}$$

The diagonal matrix $\mathbf{\Omega}(\omega)$ in eq. (21) and (22) might be called the modal receptance matrix.

We can now turn to a stationary random excitation. By applying (22) in expression (8), the displacement response CS matrix from modal superposition gets:

$$\mathbf{S}_{uu}(\omega) = \mathbf{H}(\omega)\mathbf{S}_{ff}(\omega)\mathbf{H}(\omega)^H = \mathbf{\Phi}\mathbf{\Omega}(\omega)\mathbf{\Phi}^T\mathbf{S}_{ff}(\omega)(\mathbf{\Phi}\mathbf{\Omega}(\omega)\mathbf{\Phi}^T)^H = \\ = \mathbf{\Phi}\mathbf{\Omega}\underbrace{\mathbf{\Phi}^T\mathbf{S}_{ff}\mathbf{\Phi}}_{\substack{\text{modal force}\\ \text{CS matrix}}}\mathbf{\Omega}^*\mathbf{\Phi}^T \tag{24}$$

or the displacement response CS terms between nodes (or elements) j, k as a summation:

$$S_{u_j u_k}(\omega) = \sum_{r=1}^{N_{dof}}\sum_{v=1}^{N_{dof}} H_{jr}S_{f_r f_v}H_{vk}^* = \\ = \sum_{r=1}^{N_{dof}}\sum_{v=1}^{N_{dof}}\sum_{n=1}^{N_M}\sum_{m=1}^{N_M} \frac{\varphi_j^{(n)}\varphi_r^{(n)}\varphi_v^{(m)}\varphi_k^{(m)}}{((1+i\eta)\omega_n^2 - \omega^2)((1-i\eta)\omega_m^2 - \omega^2)} S_{f_r f_v} \tag{25}$$

The modal force matrix is identified in (24) as:

$$\mathbf{S}_{f_m f_n}(\omega) = \mathbf{\Phi}^T\mathbf{S}_{ff}(\omega)\mathbf{\Phi} \tag{26}$$

Equation (24) has been applied in this work to reach a panel TBL response.

4.4 Sound transmission

The sound transmission through a TBL excited panel has in the following been simplified by the expression for sound radiation from a vibrating baffled planar source into free space. This makes it possible to apply the Reighley's integral formula which is a special case of Helmolz integral equation. While staying to finite element midpoint variables the discretisation of Reyleigh's formula becomes quite simple and effective regarding computational cost. The analysis has been assumed to be uncoupled in the sense that the air load and radiation will not influence the panel vibrations.

The Reighley's integral formula for a planar sound radiator [5]:

$$p(\mathbf{r},\omega) = \frac{i\omega\rho}{2\pi}\int_{S_0}\frac{e^{-ik|\mathbf{r}-\mathbf{r}_0|}}{|\mathbf{r}-\mathbf{r}_0|}v_z(\mathbf{r}_0,\omega)dS_0 \tag{27}$$

where: $p(\mathbf{r},\omega)$ sound pressure in an air point
$\mathbf{r}$ space vector to field point in air
$\mathbf{r}_0$ space vector to field point on vibrating surface

S_0	surface of vibrating area
v_z	surface velocity normal to panel
k	wavenumber in air
ρ	air density

In the following the TBL sound transmission will be dealt with by means of the sound power radiated from the panel (face opposite to the TBL).

Sound intensity, mean value in z-direction (normal to plate), $I_z(r)$, [14]:

$$I_z(\mathbf{r}) = \frac{1}{T}\int_0^T p(\mathbf{r},t)v_z(\mathbf{r},t)dt \tag{28}$$

alternatively, in the frequency plane (with notations introduced above):

$$I_z(\mathbf{r},\omega) = cE[Re\{p(\mathbf{r},\omega)v_z^*(\mathbf{r},\omega)\}] = Re\{S_{pv_z}(\mathbf{r},\omega)\} \tag{29}$$

where: $S_{pv_z}(\mathbf{r},\omega)$ = pressure velocity CS in space point r

apply Rayleigh's formula,(27), in (29) to express the surface intensity:

$$I_z(\mathbf{r},\omega) = cE\left[Re\left\{\frac{i\omega\rho}{2\pi}\int_{S_0}\frac{e^{-ik|\mathbf{r}-\mathbf{r}_0|}}{|\mathbf{r}-\mathbf{r}_0|}v_z(\mathbf{r}_0,\omega)v_z^*(\mathbf{r},\omega)dS_0\right\}\right] =$$

$$= Re\left\{\frac{i\omega\rho}{2\pi}\int_{S_0}\frac{e^{-ik|\mathbf{r}-\mathbf{r}_0|}}{|\mathbf{r}-\mathbf{r}_0|}S^v_{rr_0}(\omega)dS_0\right\} \tag{30}$$

where: S_0 = plate surface

$\mathbf{S}^v_{rr_0}$ = plate velocity CS (where also **r** is on the plate surface)

Re{ } denotes real part

The sound power radiated from a baffled plate, $P(\omega)$, may then be written:

$$P(\omega) = \int_S I_z(\mathbf{r},\omega)dS = \{(30)\} = Re\left\{\frac{i\omega\rho}{2\pi}\int_S\int_{S_0}\frac{e^{-ik|\mathbf{r}-\mathbf{r}_0|}}{|\mathbf{r}-\mathbf{r}_0|}S^v_{rr_0}(\omega)dS_0dS\right\} =$$

$$= Re\left\{\frac{\omega\rho}{2\pi}\int_S\int_{S_0}\frac{i\cos(k|\mathbf{r}-\mathbf{r}_0|)+\sin(k|\mathbf{r}-\mathbf{r}_0|)}{|\mathbf{r}-\mathbf{r}_0|}S^v_{rr_0}(\omega)dS_0dS\right\} =$$

$$= \frac{\omega\rho}{2\pi}\int_S\int_{S_0}\frac{\sin(k|\mathbf{r}-\mathbf{r}_0|)}{|\mathbf{r}-\mathbf{r}_0|}Re\{S^v_{rr_0}(\omega)\}dS_0dS \tag{31}$$

(the term $\int_S\int_{S_0}\frac{\cos(k|\mathbf{r}-\mathbf{r}_0|)}{|\mathbf{r}-\mathbf{r}_0|}Im\{S^v_{rr_0}(\omega)\}dS_0dS$ vanish since the argument is anti-symmetric)

Or alternatively in the discrete case, as a summation over finite element midpoints:

$$P(\omega) \approx \frac{\omega\rho}{2\pi}\left(2\sum_{j=2}^{N_E}\sum_{k=1}^{j-1} \frac{\sin\left(k\left|r_j - r_k\right|\right)}{\left|r_j - r_k\right|} A_j A_k \, Re\left(S_{jk}^{v}(\omega)\right) + \sum_{j=1}^{N_E} kS_{jj}^{v}(\omega) A_j^2 \right) \quad (32)$$

where:
- k = wave number (in air)
- N_E = total number of finite elements
- j, k = finite element indices (related to S and S_0 respectively)
- A_j, A_k = finite element areas
- $S_{jk}^{v}(\omega)$ = plate velocity cross-spectrum between FE number n and m
- ρ = air density

Diagonal (singularity) - terms has to be treated separately in the discrete case as seen in (32). All presented results are given by equation (32), with $S_{jk}^{v}(\omega)$ from (24).

4.5 Normalised transmitted sound power

Presented results from analyses of transmitted sound power, TP(ω), are in the following normalised regarding to the TBL pressure auto spectrum like:

$$TP(\omega) = \frac{\omega m P(\omega)}{A\Gamma_{pp}(\omega)} \quad (33)$$

where:
- P radiated sound power, see eq.(32)
- Γ_{pp} pressure auto spectrum, see eq.(1)
- m is the panel mass/area (=ρh)
- A is the panel area

By applying this normalisation narrow band and wide band results can be compared against the same y-axis level and we can leave out the question of TBL pressure auto spectrum model.

5 Needed number of operations

5.1 Straight forward approach

With the chosen basic equations stated above we may take a look at the computational cost in order to reach the transmitted sound power from a TBL. The computational cost is given in Table 1 below in terms of the needed number of operations in each calculation step, for the direct FE and the FE/Modal approach respectively. The number of operations given represents the clearly dominating part of the cost. For steps 3 and 6, force CS and transmitted sound power: 'one operation' involves some function evaluations while for other steps 'one operation' = one multiplication + one addition.

Table 1. Needed number of operations in FE-based TBL response analysis

ANALYSIS STEP	Eq.no.		NUMBER OF OPERATIONS	
	Direct FE	Modal	DIRECT FE	FE/MODAL
1. Eigenvalue Analysis	-	-	*(not needed)*	$w^2N_{dof}+80wN_{dof}N_M+84N_{dof}N_M^2$
Creation of:	*below: at each frequency step*			
2. FRF-matrix, H(ω)	11	(22)	$w^2N_{dof}+wN_{dof}^2$	*(H(ω) creation implicit in step 4+5)*
From step 3 and on: finite element midpoint based variables and expressions applied				
3. Force CS matrix	9	9	N_E^2	N_E^2
4. Modal force CS matrix	-	26	*(not needed)*	$N_MN_E^2+N_M^2N_E$
5. Panel CS-resp. matrix	8	24	$2N_E^3$	$N_MN_E^2+N_M^2(N_E+2)$
6. Radiated Power	32	32	N_E^2	N_E^2

Where: N_{dof} = number of degrees of freedom
w = half bandwidth (bandwidth=2w+1)
N_E = number of finite elements
N_M = number of included modes

The cost for the eigenvalue solver is taken from [6] and is valid for a blocked Lanzos algorithm. This number can be slightly different depending on code and input parameters but is believed to give a good estimate in this context. Comparing the given cost for the eigenvalue analysis, which has to be carried out only once, with the cost for FRF-matrix inversion in the Direct FE approach (step 2) shows that the costs are about the same order. The FRF-matrix inversion though has to be made at each frequency step. In a typical TBL analysis one would have to cover hundred or thousands frequencies, which would of course make step 2 much more costly. Looking further

down in the calculation process we find that step 5, for the Direct FE approach, might be even more costly than step 2 (depending on bandwidth and order of FE-elements) with $2N_E^3$ operations. In the case of a Modal approach these most costly steps becomes significantly reduced while we can expect: $N_M << N_E$. The most important conclusions from Table 1 are:

- A Modal/FE approach can be expected to be by far more effective than a direct FE approach in terms of computational cost.

- The limiting steps towards a prediction of TBL induced transmitted sound power with a Modal/FE approach can be expected to be the creations of modal force CS matrix and panel response CS matrix respectively.

- Both these two steps have to be focused on when searching for better computational efficiency in the FE/Modal approach.

5.2 Standard ways to reduce the number of operations in a Modal/FE approach

One usual way to reduce the computational cost is to assume that modal cross terms in (24, 25) can be excluded for lightly damped systems. Equation (25) then goes to:

$$S_{u_j u_k}(\omega) = \sum_{r=1}^{N_{dof}} \sum_{v=1}^{N_{dof}} \sum_{n=1}^{N_M} \frac{(\varphi_j^{(n)} \varphi_k^{(n)})^2}{(\omega_n^2 - \omega^2)^2 + (\eta \omega_n^2)^2} S_{f_r f_v} \tag{34}$$

Instead of a N_M x N_M sized modal force CS matrix (eq.26) we now get a N_M x 1 modal force CS vector. The gain in computational cost related to the introduced simplification is rather small though, since the dominating $N_M N_E^2$ operations for the $\mathbf{\Phi S}_{ff}$ multiplication is needed whether modal cross-terms are included or not. The needed number of operations for step 4 and 5 in Table 1 reduces only from $N_M N_E^2 + N_M^2 N_E$ $(+2N_M^2)$ to $N_M N_E^2 + N_M N_E$ $(+2N_M)$ when excluding modal cross terms.

6 Basic principles and implementation of the Semi-Random FE/Modal approach

Knowing that the matrix multiplications following the eigenvaluanalysis represents the "bottle neck" in the path from a FE/Modal model to a transmitted sound power prediction, these steps where examined with the aim to find more cost effective techniques. An approach found to be cost effective, and at the same time capable to produce results with sufficient and controllable accuracy, is outlined in the following. The approach is herein called Semi-Random FEM approach or SR-FEM. The fundamental characteristics of this approach are:

a. *Only a limited subset of all the finite element field variables composing the FE-model are involved in the summations (matrix multiplications) following the eigenvalue analysis*

b. *A new subset of field variables are created at each frequency of the analysis by a random sampling among the full set of (TBL excited/radiating) finite elements*

c. *The accuracy is poor (for a relatively low number of sampled elements) at each specific frequency, but after summation into 1/3-octave bands the accuracy can be kept around 1dB within each band, dependent of underlying frequency discretisation and material damping.*

d. *The CPU time gain, compared with "full" matrix multiplications, could be several hundred times and possibly more if an accuracy of ca 1.5dB is found acceptable*

e. *Based on basic probability theory well established means for error estimation can be applied*

The procedure with the SR approach is in short as follows:

At each frequency:

(1) Two independent random vectors of finite element numbers, $\mathbf{a}_1$ and $\mathbf{b}_1$ are generated. The length of vectors $\mathbf{a}_1$ and $\mathbf{b}_1$ is N_R, $N_R << N_E$ (finite element midpoint related variables assumed). An advantage is reached here if finite element numbers are sampled without replacement.

(2) Then, when creating the modal force CS (eq.26), instead of the full representation of the TBL force CS matrix (eq.9) and the modal base matrix (eq.15,16), corresponding reduced size matrices, $\mathbf{S}_{ff}^{R}$ and $\mathbf{\Phi}^{R}$, defined by the finite element sets $\mathbf{a}_1$ and $\mathbf{b}_1$ are applied. I.e. two independent modal base matrices reduced from size $N_E \cdot N_M$ to $N_R \cdot N_M$, and a force CS matrix reduced from $N_E \cdot N_E$ to $N_R \cdot N_R$. After a scaling related to the reduced number of summation terms, we now get an approximate to the modal force CS matrix, $\mathbf{S}_{f_m f_n}^{R}(\omega) \approx \mathbf{S}_{f_m f_n}(\omega)$.

(3) In the next step, two new independent random N_R-vectors of finite element numbers, $\mathbf{a}_2$ and $\mathbf{b}_2$, are generated. These two vectors are used to constitute two new reduced modal base matrices. These two matrices gives now the approximate panel response CS, together with the modal receptance matrix, $\mathbf{\Omega}(\omega)$, and the approximated modal force CS matrix $\mathbf{S}_{f_m f_n}^{R}(\omega)$ the same way as seen in equation 24 for the "Exact" or full matrix approach. The

approximate panel response CS matrix, $\mathbf{S}_{uu}^{R}(\omega)$, becomes reduced in size, $N_R \cdot N_R$ instead of the full $N_E \cdot N_E$ size.

(4) This reduced size panel response CS matrix is then applied to form the approximate sound power radiation from the panel for the frequency of concern. See equation (32). Also here a scaling related to the reduced number of summation terms is needed.

After frequency loop:

(5) These narrow band estimates of sound power are summed into 1/3-octave band levels. By using new mutually independent $\mathbf{a}_1$, $\mathbf{b}_1$, $\mathbf{a}_2$, and $\mathbf{b}_2$ vectors at each frequency, in steps (2)-(4), we also get estimates of radiated sound power independent between frequencies.

(6) The steps outlined above are then looped a number of times (N_{Loop}) in order to get final 1/3-octave mean value estimates, plus an estimation of the variance of these mean values.

The reasons to why these reduced matrices could give a "good enough" approximation of the searched response are believed to be:

- Matrix multiplications are equivalent to specific summations
- These (full) summations can be regarded as a calculation of the arithmetic mean value times the number of terms squared, for example the modal force CS terms from equation (26):

$$S_{f_m f_n}(\omega) = \varphi_m^T \mathbf{S}_{ff}(\omega)\varphi_n = \sum_j^{Ne}\sum_k^{Ne} \varphi_j^{(m)}\varphi_k^{(n)} S_{jk} = N_E^2 \frac{1}{N_E^2}\sum_j^{Ne}\sum_k^{Ne} \varphi_j^{(m)}\varphi_k^{(m)} S_{jk} =$$

$$= N_E^2 E(\varphi_j^{(m)}\varphi_k^{(m)} S_{jk}) = N_E^2 m_{mn}(\omega) \qquad (35)$$

where m_{mn} denotes the arithmetic mean of the individual m,n terms

- When one randomly pick a subset of terms from a population and sum those together, this is equivalent to calculate the estimated mean value of the full population and multiply this with the number of random terms squared,

$$S_{f_m f_n}^R = N_E^2 m_{mn}^e = N_E^2 \frac{1}{N_R^2}\sum_j^{N_R}\sum_k^{N_R} \varphi_j^{(m)}\varphi_k^{(m)} S_{jk} \approx S_{f_m f_n} \qquad (36)$$

where m_{mn}^e is the estimated mean of the individual m,n terms

- All summations, i.e. those in step 3 to 6 in table 1 and the summation into 1/3-octave bands, constitutes summations of equally distributed random variables which in each step produces a gauss distributed sum (Central limit theorem [8])

7 Needed number of operations with the SR-FEM

We may recall the needed number of operations for a standard FE/modal approach, when going from a TBL CS to interior sound pressure, approximating this number with the dominating step 4 and 5 (and calling this number "NOP_{Exact}"):

$$NOP_{Exact} \approx 2(N_M N_E^2 + N_M^2 N_E) \tag{37}$$

From the outline of the SR-FEM approach we get an approximated needed number of operations as for the SR-FEM approach:

$$NOP_{SR} \approx 2N_{Loop}(N_M N_R^2 + N_M^2 N_R) \tag{38}$$

e.g. a strong reduction if $N_R << N_E$ and N_{Loop} could be kept small enough.

It should be noted that these numbers holds for the same number of frequencies computed. And further, that the cost for setting up the modal base (the eigenvalue solution) has to be carried out in both cases (+ that this number has to be added to (37) or (38) in order to get an estimate of the total number of operations).

8 Test case

A straight forward FE/modal as well as a SR-FEM analysis was run.on a test case with the following inputs

Table 2. Input data for panel and TBL

Panel data:		**TBL (Corcos model data):**	
Length:	0.768 m	α_1:	0.116
Width:	0.328 m	α_2:	0.7
Thickness:	1.6 mm	U_∞:	120 and 240 m/s
Youngs modulus:	7.0E10 Pa	U_C:	0.8 U_∞
ν:	0.33	ρ_{air}:	1.2 kg/m^3
ρ_{Al}:	2700 kg/m^3	c:	340 m/s
$\eta,\eta(\omega)$=constant:	0.02	(ρ_{air} and c the same on each side of panel)	

Modal panel model:	
Number of included modes:	97
Number of finite elements:	1344
Upper frequency limit:	2000 Hz

9 Results

In Figure 2 results of normalised transmitted sound power for the given test example are shown, both for the standard modal/FE (called "Exact" in Figure 2) and for the SR-FEM approach (called "Random" in Figure 2). The number of sampled finite elements, N_R, was in this case 304 (out of 1344 elements in total)

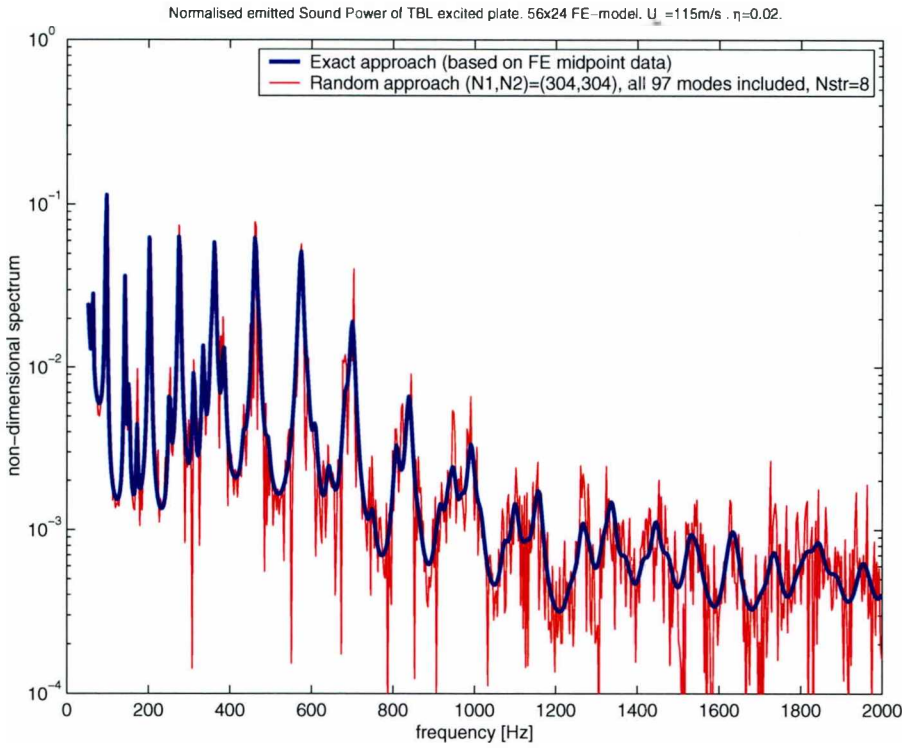

Figure 2. Example of narrowband results of transmitted sound power for standard and SR-FEM method
comment: Nstr denotes a kind of grouping of samples, stratified sampling, in this case into 8 sections of the panel

As seen in Figure 2 the SR-FEM results shows a noise-like behaviour around the "exact" results. By going to wide-band results, in this case 1/3-octave bands, outgoing from these narrowband results we get the results shown in Figure 3 below:

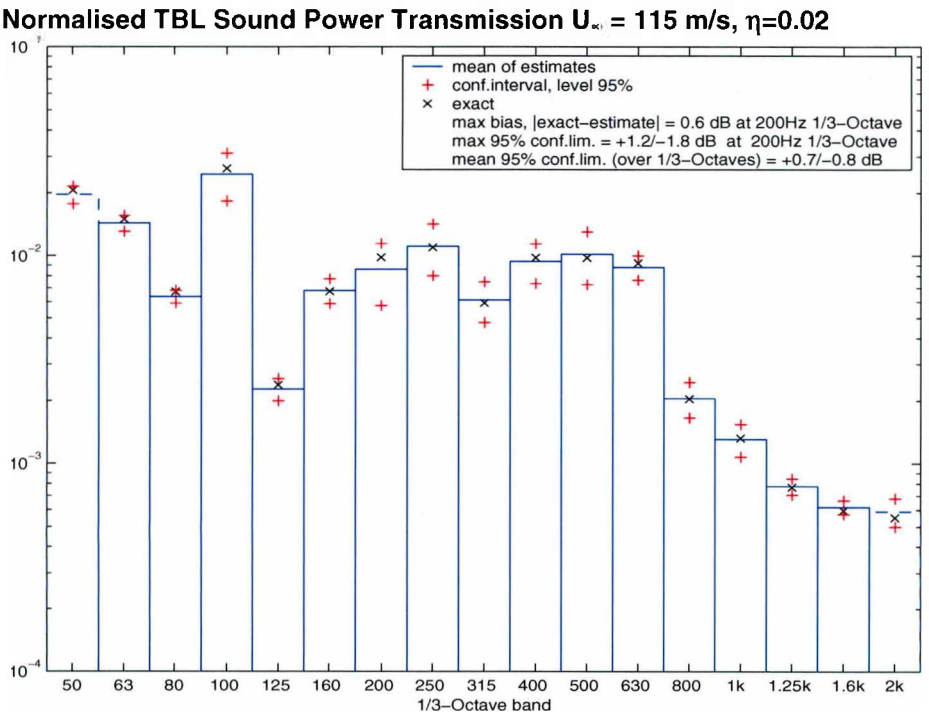

Figure 3. Ex.1 of 1/3 octave band results of transmitted sound power for standard and SR-FEM method

In the 1/3-octave band results we see that SR-FEM (blue line bars) approximates standard modal/FE (called "exact" and denoted with a black "x" in Figure 3) quite well. Together with estimated levels are also confidence levels estimated. Upper and lower levels of 95% confidence intervals are shown as red "+"-signs. In this case we see that all 1/3-octave SR-FEM estimates are found within these confidence intervals. Further the maximum bias found in any band 0.6 dB, maximum 95% confidence interval +1.2/-1.8 dB and a mean 95% confidence interval found as +0.7/-0.8 dB. We may also note that the variation along frequency axis is found quite even, which means that a equidistant frequency discretisation is appropriate.

For the same case, but with a higher structural damping , η=0.10, the variation reduces and we get:

Max bias=0.2 dB, maximum 95% confidence interval=+0.7/-0.9, and the mean 95% confidence interval to be +0.5/-0.5 dB. See Figure 4 below.

In order to get final 1/3 octave levels and variance estimates of these, the complete frequency loop is as mentioned earlier gone through a number of times (N_{Loop}). Confidence intervals , I_m, for achieved 1/3 octave levels are then given as, [8]:

$$I_m = (m^e - t_{\alpha/2}(v)D, m^e + t_{\alpha/2}(v)D) \tag{39}$$

where:

m^e is the estimated 1/3 octave mean

$t_{\alpha/2}(v)$ is the t-distribution for v (i.e. $\alpha = 0.025$ for 95% confidence level)

$v = N_{Loop}-1$, number of samples-1 or degrees of freedom for the t-distribution

$D = d_{N_R}\sigma^e / \sqrt{N_{Loop}}$, with σ^e = 1/3-octave level sample standard deviation

$d_{N_R} = \sqrt{(N_E - N_R)/(N_E - 1)}$, correction factor for finite population of FE:s

Confidence intervals in decibels are then defined by: $I_{L_m} = 10log(I_m / m^e)$ (40)

It could be emphasized here that error estimates given by (39), and exemplified in Figure 3 and 4, where found to agree well with expected error bounds. I.e., seen over a larger set of runs, for the 95% confidence interval case, 95% of the "exact" FE 1/3-octave band levels tend to be found within these bounds and 5% outside. These results are not presented in any more detail in this paper, but from the two sample results given in Figure 3 and 4 we see that: 1 out of in total 34 individual 95% confidence intervals happens to not include the "exact" FE result (80 Hz 1/3-octave in Figure 3). That is slightly better than the expected 1 out of 20 result that we would get in the long run.

Normalised TBL Sound Power Transmission U_∞ = 115 m/s, η=0.10

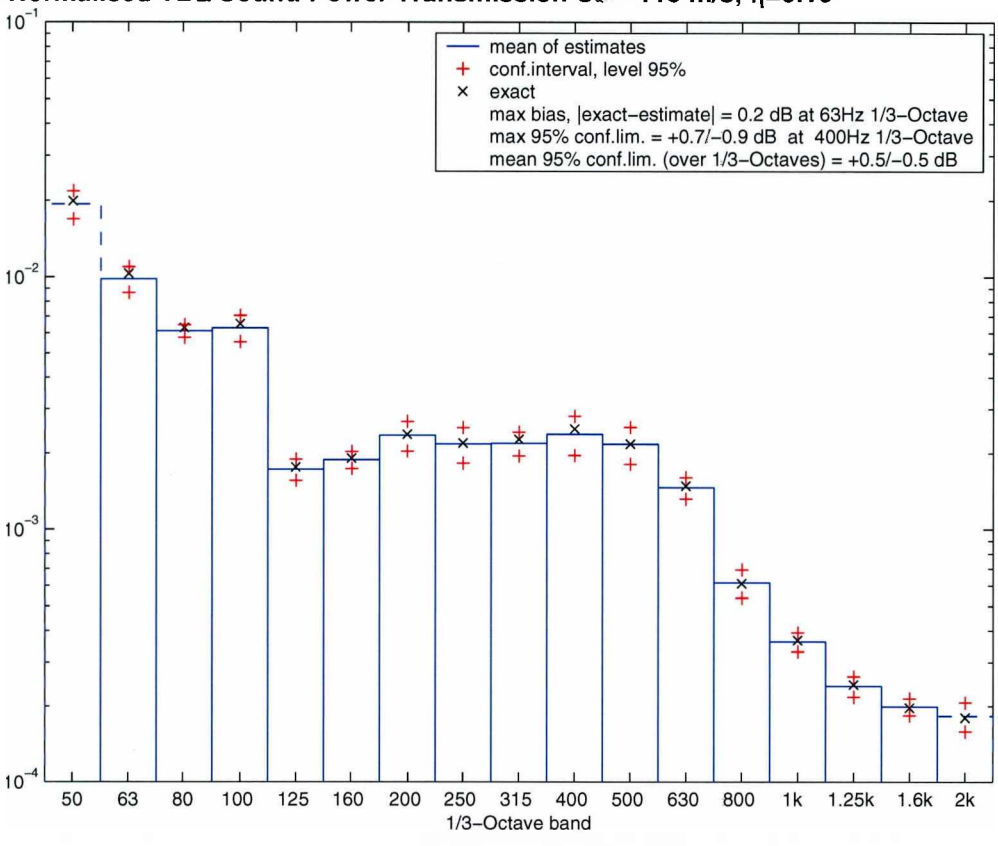

Figure 4. Ex.2 of 1/3 octave band results of transmitted sound power for standard and SR-FEM method

10 CPU-time gain with SRD

The actual CPU-times reached on the used platform for different discretisations of the previously described panel (see Table 2) are showed in Figure 5. It is important to note here that the accuracy of the SR-FEM is ca 1.5 dB within 1/3-octave bands compared with the "Exact" approach. And that this accuracy is defined as the maximum upper 95% confidence limit found among 1/3-octaves. The eigenvalue analyses were carried out with NASTRAN [9]. In the figure 'circle' denotes CPU-time when applying 20-node quadratic solid finite elements, HEX20. And 'square' denotes CPU-time for 4-node linear shell elements, QUAD4 (all previously shown spectra are reached with HEX20 elements). As seen in Figure 5 matrix multiplications/summations with SR-FEM (remember 1.5 dB accuracy) becomes less costly than the eigenvalue solution even when QUAD4-elements are applied. In the studied 4 kHz case the CPU-time gain for the complete path, eigenvalue analysis (QUAD4) + matrix multiplications/summations, is found to be around 50 times with SR-FEM approach compared with the "Exact" modal/FEM approach. The number of frequencies originally computed for both the "Exact" and SR-FEM are the same for each of the three panel models.

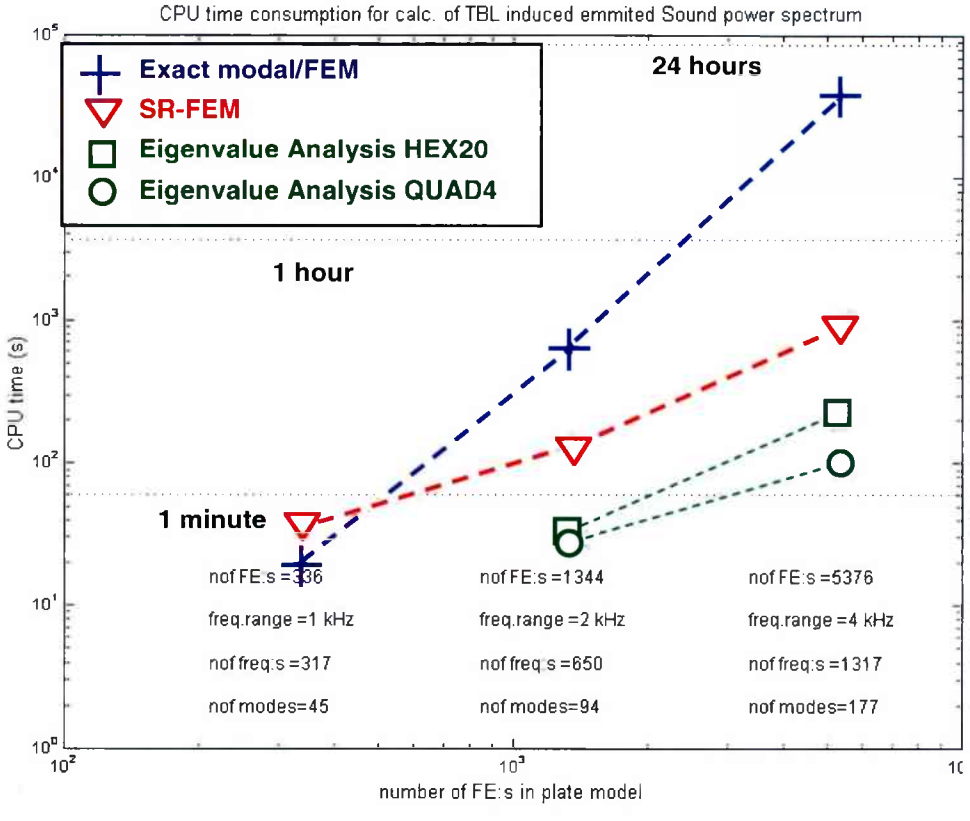

Figure 5. Comparison of CPU-times for standard and SR-FEM method

Further, in Figure 5 we could see that CPU-times for the SR-FEM solution part seem to follow the eigenvalue solution CPU-times with increasing model size. For the two studied cases, 1344 FE's/f_{max}=2kHz and 5376 FE's/f_{max}=4kHz respectively, we find an increase in CPU-time with around a factor of 5 between eigenvalue solution and the SR-FEM step. This could be compared with the very strong CPU-time increase of the 'Exact' modal FEM with model size/upper frequency limit.

11 Conclusions

A way to significantly reduce the computational effort for finite element based prediction of TBL induced sound transmission is presented. The, herein called, SR-FEM approach shows in given examples CPU time gains of the order of 50 times compared with a straight forward finite element midpoint modal approach for results presented in 1/3-octaves.

The proposed method is based on fundamental probability theory, which brings about well defined means for error estimation. The SR-FEM accuracy, versus standard modal/FEM, is in the presented cases ca 1.5 dB within in 1/3-octave bands. A higher material damping, or other energy dissipation effect leading to less pronounced resonance peaks, gives a higher accuracy – or a possibility to smaller computational effort. Further, by choosing a wider presentation frequency bandwidth, e.g.. octave bands, gives a higher accuracy (or lower CPU-time with the same accuracy).

In contrary to a standard modal/FEM approach, where the computational effort following upon the eigenvalue analysis is by far the most costly part, the SR-FEM approach turns these two computational blocks to be about the same order of size in terms of CPU-time. This means that the question:

"Would a TBL sound transmission study on a large structure/FE-model at hand be affordable, regarding computer time and memory?"

relay solely on weather the initial eigenvalue solution is reachable or not. If an eigenvalue solution is affordable, the computer resources will also be sufficient for a stationary random TBL response analysis (typically in 1/3 octave bands with a quantified and limited error bound).
Thus we have completely new situation regarding upper limit in model size, as well as in judging this limit, thanks to the SR-FEM.

A logarithmic bandwidth, such as for the studied plate case, is found appropriate in order to give an even accuracy along the frequency axis. This is achieved while the number of sampled elements is kept constant across all frequencies. For other structures or cases, with a different distribution of resonances a frequency dependent sampling might be advantageous.

The SR-FEM approach could most probably also be applicable for other random excitations, such as diffuse sound fields. Even in these cases it is expected to give significant time gains compared with conventional FE/Modal methods, still with an error estimate based on fundamental statistics.

References

1. ENABLE/EU Research Program – FP5 n° G4RD-CT-2000-00223

2. Corcos G.M., Resolution of Pressure in Turbulence, JASA, 35 (2) 1963

3. Wirsching P.H., Random Vibrations: Theory and Practice, John Wiley Sons, Inc.1995 ISBN 0-471-58579-3

4. Clough R.W., Penzien J., Dynamics of Structures, McGraw-Hill 1975, ISBN 0-07-085098-4

5. Fahy F., Sound and Structural Vibration, Academic Press Inc. ISBN 0-12-247670-0

6. J. Bathe, Finite Element Procedures, Prentice Hall 1996, ISBN 0-13-301458-4

7. Clough R.W., Penzien J., Dynamics of Structures, McGraw-Hill 1975, ISBN 0-07-085098-4

8. G. Blom, Sannolikhetsteori och statistikteori med tillämpningar Bok C, Studentlitteratur 1998, ISBN 91-44-03594-2

9. UAI/NASTRAN 20.0 User's Guide, fifth edition 1997